Title

Abnormal phase discontinuity of alpha- and theta-frequency oscillations in schizophrenia.

Authors

Koshiyama, Daisuke

Miyakoshi, Makoto

Tanaka-Koshiyama, Kumiko

et al.

Publication Date

2021-05-01

DOI

10.1016/j.schres.2021.03.007

Peer reviewed

HHS Public Access

Author manuscript

Schizophr Res. Author manuscript; available in PMC 2022 May 01.

Published in final edited form as:

Schizophr Res. 2021 May ; 231: 73–81. doi:10.1016/j.schres.2021.03.007.

Abnormal phase discontinuity of alpha- and theta-frequency oscillations in schizophrenia

Daisuke Koshiyama, M.D., Ph.D.[1], **Makoto Miyakoshi, Ph.D.**[2], **Kumiko Tanaka-Koshiyama, M.D.**[1], **Yash B. Joshi, M.D., Ph.D.**[1,3], **Joyce Sprock, B.A.**[1,3], **David L. Braff, M.D.**[1,3], **Gregory A. Light, Ph.D.**[1,3]

[1]Department of Psychiatry, University of California San Diego, La Jolla, CA, USA

[2]Swartz Center for Neural Computation, University of California San Diego, La Jolla, CA, USA

[3]VISN-22 Mental Illness, Research, Education and Clinical Center (MIRECC), VA San Diego Healthcare System, San Diego, CA, USA

Abstract

Background: Schizophrenia patients have abnormal electroencephalographic (EEG) power over multiple frequency bands, even at rest, though the primary neural generators and spatiotemporal dynamics of these abnormalities are largely unknown. Disturbances in the precise synchronization of oscillations within and across cortical sources may underlie abnormal resting-state EEG activity in schizophrenia patients.

Methods: A novel assessment method was applied to identify the independent contributing sources of resting-state EEG and assess the phase discontinuity in schizophrenia patients (N=148) and healthy subjects (N=143).

Results: A network of 11 primary contributing sources of scalp EEG was identified in both groups. Schizophrenia patients showed abnormal elevations of EEG power in the temporal region in the theta, beta, and gamma-bands, as well as the posterior cingulate gyrus in the delta, theta, alpha, and beta-bands. The higher theta-band power in the middle temporal gyrus was significantly correlated with verbal memory impairment in patients. The peak frequency of alpha was lower in patients in the cingulate and temporal regions. Furthermore, patients showed a higher rate of alpha phase discontinuity in the temporal region as well as a lower rate of theta phase discontinuity in the temporal and posterior cingulate regions.

Corresponding Author: Makoto Miyakoshi, Ph.D., Swartz Center for Neural Computation, University of California San Diego, 9500 Gilman Drive, La Jolla, CA, USA 92093-0559, Tel.: (858) 822-7534, mmiyakoshi@ucsd.edu.

Author contributions

J. Sprock and G. Light collected the data. D. Koshiyama, M. Miyakoshi, and K. Tanaka-Koshiyama analyzed the data. M. Miyakoshi wrote the Matlab code. D. Koshiyama, M. Miyakoshi, K. Tanaka-Koshiyama, Y. Joshi, D. Braff and G. Light interpreted the results. D. Koshiyama, M. Miyakoshi and G. Light designed the study. G. Light supervised all aspects of collection, analysis, and interpretation of the data. D. Koshiyama, M. Miyakoshi and G. Light wrote original manuscript. K. Tanaka-Koshiyama, Y. Joshi, J. Sprock and D. Braff reviewed and edited the manuscript. All authors contributed to and approved the final manuscript.

Conflict of Interest

G.A. Light reported consulting for Astellas Pharma, Inc, Heptares Therapeutics, NeuroSig, Neurocrine, and Novartis.

Conclusions: Abnormal rates of phase discontinuity of alpha- and theta-band, abnormal elevations of EEG power in multiple bands, and a lower peak frequency of alpha were identified in schizophrenia patients at rest. Clarification of the mechanistic substrates of abnormal phase discontinuity may clarify core pathophysiologic abnormalities of schizophrenia and contribute to the development of novel biomarkers for therapeutic interventions.

Keywords

Resting-state electroencephalography (EEG); Phase discontinuity; Source level analysis; Schizophrenia; Alpha oscillation; Theta oscillation

1. Introduction

Neural oscillations play an essential role in the cortico-cortical transmission and the integration of information across neural networks supporting various brain functions, such as perception, attention, and cognition (Galuske et al., 2019; Hagoort et al., 2004; Joliot et al., 1994; Miltner et al., 1999; Rodriguez et al., 1999; Spellman et al., 2015; Traub et al., 1996). These oscillations, resulting from the coordinated and rhythmic firing of ensembles of neurons, are defined by the frequency characteristics of electroencephalogram (EEG) recordings.

Schizophrenia patients have significantly increased EEG activity at rest spanning the majority of the frequency spectrum (Tanaka-Koshiyama et al., 2020), including theta-, alpha-, beta- (Newson and Thiagarajan, 2018) and gamma-bands (Bandyopadhyaya et al., 2011; Baradits et al., 2019; Tikka et al., 2014). Resting-state EEG is considered a promising candidate biomarker for investigating the pathophysiology of schizophrenia and advancing novel therapeutic development (da Cruz et al., 2020; Hirano et al., 2015). We recently found that schizophrenia patients show “hyper-connectivity” of gamma-band activity across a distributed network of frontal, temporal, and occipital sources in schizophrenia patients (Koshiyama et al., 2020).

These observations indicate that broad abnormalities are evident in the flow of spectral information across networks of cortical sources, even at rest. Methods for characterizing the temporal phase dynamics within and across frequency bands that improve the understanding of the pathophysiology of schizophrenia are needed. One emerging method to characterize temporal phase dynamics includes assessing phase discontinuity. In neuropsychiatric disorders, waveform amplitudes and shapes in spontaneous EEG may be driven by seemingly stochastic spiking, perhaps attributable to increased biological noise, reduced signal, and/or disrupted neural circuit function (Uhlhaas and Singer, 2010). Conceivably, discontinuities may be recurrent, and waveform irregularities may be prolonged, which disrupts the fluid coordination of neural information processing. To date, phase discontinuity has been described in healthy subjects participating in an EEG sleep study, as reported in a study by Sanders (2019). In the study, smooth behavioral transitions across activity states such as waking up vs. falling asleep were accompanied by smooth transitions between high and low rates of phase discontinuity. Interestingly, older individuals had increased phase discontinuity compared to younger participants. These data have added support for the

hypothesis that phase discontinuities and abnormal waveforms are related and that excessive fluctuations in phase discontinuity may reduce efficiency for brain functioning. Such fluctuations may lead to diminished signal-to-noise, abnormal signal propagation, and ultimately disruption of healthy brain circuitry.

To our knowledge, no previous studies have assessed phase discontinuity in patients with neuropsychiatric disorders. In this study, a novel method was developed and applied to identify the key independent contributing sources of resting-state EEG as well as assess the phase discontinuities across independent cortical sources of resting-state EEG in schizophrenia patients and healthy comparison subjects. Furthermore, exploratory correlation analyses of cognitive dysfunction with abnormal phase discontinuity rates and EEG power were conducted in schizophrenia patients. We hypothesized that patients with schizophrenia would show abnormal frequency-specific phase discontinuity across cortical networks.

2. Material and methods

2.1. Subjects

EEG data from N=147 healthy comparison subjects and N=159 schizophrenia patients was processed. Recordings from N=2 healthy comparison subjects and N=5 schizophrenia patients were dropped in the quality control step in the preprocessing of EEG. For quality control of group-level analysis for independent component clustering, the data from N=2 healthy comparison subjects and N=6 schizophrenia patients were removed. Therefore, we used a final sample of N=143 healthy comparison subjects and N=148 schizophrenia patients in the statistical analysis (Table 1, Supplementary Method 1).

Verbal memory performance was assessed via the California Verbal Learning Test second edition (CVLT-II), using total correct scores from the Total Learning (list A trials 1–5; Delis et al., 2000). Working memory was evaluated using Letter-Number Sequencing (Crowe, 2000). For both cognitive measures, higher scores indicate better performance, and standard scores were employed. Written informed consent was obtained from each subject via The Institutional Review Board of University of California San Diego approved procedures (071831, 170147). As shown in Table 1, the groups differed in age ($t_{289} = 4.7$, $p = 4.7\times10^{-6}$) and sex distribution ($\chi^2 = 10.3$, $df = 1$, $p = 1.3\times10^{-3}$).

2.2. Scalp EEG recording

Resting-state spectral characteristics assessed at the scalp level, and effective connectivity analyses were described previously (Koshiyama et al., 2020; Tanaka-Koshiyama et al., 2020). Participants sat in a comfortable chair in a quiet room and were instructed to relax and with their eyes open during the session. Subjects were closely monitored to ensure that subjects remained awake. EEG recordings were set for at least 3 minutes across all participants. EEG was continuously digitized at a rate of 1000 Hz (nose reference, forehead ground) using a 40-channel Neuroscan system (Neuroscan Laboratories, El Paso, Texas). The electrode montage was based on standard positions in the International 10–5 electrode system (Oostenveld and Praamstra, 2001) fit to the Montreal Neurological Institute (MNI)

template head used in EEGLAB (Collins et al., 1994), including AFp10 and AFp9 as horizontal electro-oculographic (EOG) channels, IEOG and SEOG above and below the left eye as vertical EOG channels, Fp1, Fp2, F7, F8, Fz, F3, F4, FC1, FC2, FC5, FC6, C3, Cz, C4, CP1, CP2, CP5, CP6, P7, P3, Pz, P4, P8, T7, T8, TP9, TP10, FT9, FT10, PO9, PO10, O1, O2, and Iz. Electrode-to-skin impedance mediated by conductive gel was brought below 4 kΩ. The system acquisition bandpass was 0.5–100 Hz.

2.3. EEG preprocessing

EEG data were imported to EEGLAB 14.1.2 (Delorme and Makeig, 2004) running under Matlab 2017b (The MathWorks, Natick, MA). Data were high-pass filtered [finite impulse response (FIR), Hamming window, cutoff frequency 0.5 Hz, transition bandwidth 0.5]. EEGLAB plugin *clean_rawdata()* including Artifact Subspace Reconstruction (ASR) was applied to reduce high-amplitude artifacts (Blum et al., 2019; Chang et al., 2018, 2020; Gabard-Durnam et al., 2018; Kothe and Makeig, 2013; Mullen et al., 2015). The parameters used were: flat line removal, 10 s; electrode correlation, 0.7; ASR, 20; window rejection, 0.5. Mean channel rejection rate was 4.3 % (standard deviation (SD) 3.2, range 0–18.4). Mean data rejection rate was 0.9% (SD 2.6, range 0–40.0). The rejected channels were interpolated using EEGLAB's spline interpolation function. Data were re-referenced to average. Adaptive mixture independent component analysis (ICA) was applied to the preprocessed scalp recording data to obtain temporally maximally independent components (ICs). For scalp topography of each IC derived, equivalent current dipoles were estimated using Fieldtrip functions (Oostenveld et al., 2011; Figure 1). For scalp topographies, two symmetrical dipoles were estimated (Piazza et al., 2016). To select brain ICs among all types of ICs, EEGLAB plugin *ICLabel()* was used (Pion-Tonachini et al., 2019). The inclusion criteria were: 'brain' label probability > 0.7; residual variance i.e., var((actual scalp topography) − (theoretical scalp projection from the fitted dipole))/var(actual scalp topography) < 0.15. Seven subjects were removed because they did not have a minimum of 4 ICs. Mean number of ICs that remained was 12.5 (SD 4.5, range 4–25). Mean data length was 327.5 s (SD 43.9, range 183–600).

2.4. Group-level independent component clustering

A total of 3740 brain ICs obtained from 299 subjects were submitted for clustering analysis using Talairach coordinate values of the associated equivalent current dipoles. k-means clustering with the Silhouette index (Rousseeuw, 1987) indicated the optimum number of brain IC clusters was 11.

The abovementioned preprocess using *clean_rawdata()* rejects data windows if the ASR result does not meet the clean-data criterion defined by the self-constructed calibration data. Such a window rejection creates discontinuous points called boundary, which may introduce high-frequency artifact as a Fourier transform of an impulse/step function shows high-frequency harmonics. Thus, epochs containing boundaries were excluded from the subsequent time-frequency decomposition. The group-mean number of boundaries was calculated, which was 1.8 boundaries per dataset (SD 3.57, range 0–37). For quality control, we rejected subjects with more than 10 boundaries. As a result, 8 subjects were removed. In addition, 2 additional ICs were removed at this stage because their dipole locations were

outside the brain. Thus, 3663 ICs from 291 subjects were finally selected and submitted to the next process.

2.5. EEG band power in estimated source locations.

For each time series of IC activation, power spectral density (PSD) was calculated using Welch's method implemented in EEGLAB function *spectopo()*. The parameters used were: window type, Hamming; window length, 1 s; window overlap, 50%; frequency resolution, 0.1 Hz. This relatively high-frequency resolution is for subsequent alpha-band peak frequency analysis. PSD in 541 frequency bins from 1 to 55 Hz was averaged into the following conventional EEG frequency bands: Delta, 1–4 Hz; Theta, 4–8 Hz; Alpha, 8–13 Hz; Beta, 13–30 Hz; Gamma, 30–50 Hz. The mean PSD of the 5 frequency bands were calculated for 11 IC clusters, and there were two groups, thus generated 4-D tensor of data 11 × 5 × 2 × (number_of_ICs) where the length of the data in the last term varies for each group and IC cluster. After calculating this frequency-band separated PSD data structure, group differences were tested to generate 11 (clusters) × 5 (frequency bands) result matrix.

2.6. Phase Discontinuity Index

Phase discontinuities between 1–55 Hz were quantified as follows. The complex continuous 1-D wavelet transform (CWT) implemented in Matlab *cwt()* was applied using the following parameters: Wavelet type, Morse (Olhede and Walden, 2002); Symmetry parameter gamma, 3; Time-bandwidth product, 60. Starting from the Nyquist frequency (500 Hz), down to 8 octaves below (around 2 Hz) were analyzed. There were 20 voices per octave. Frequency bins below 52 Hz were selected for the final analysis, leaving 99 frequency bins of interest from 2–52 Hz at each time sample. The obtained complex Wavelet transform data were segmented into 5-s epochs. Let i-th epoch be the complex data $x_i(f)$. Phase discontinuity was calculated as follows. First, phase coherence between i-th and i+1-th epoch was calculated (Nolte et al., 2004).

$$C_{i,i+1}(f) = \frac{S_{i,i+1}(f)}{\left(S_{i,i}(f)S_{i+1,i+1}(f)\right)^{1/2}}$$

where $S_{i,i+1}(f)$ is a cross spectrum between $x_i(f)$ and $x_{i+1}(f)$

$$S_{i,i+1} = x_i(f)x^*_{i+1}(f)$$

where * represents a complex conjugate. The time-frequency phase matrix $\theta(t, f)$ was calculated using coherence for all epochs (Sanders, 2019).

$$\theta(t,f) = \tan^{-1}\frac{\mathrm{Im}\left(C_{i,i+1}\right)}{\mathrm{Re}\left(C_{i,i+1}\right)}$$

To detect phase change over short time interval, time-frequency matrix of phase difference $\Delta\theta$ was calculated as follows.

$$\Delta\theta(t, f) = \theta(2, f) - \theta(1, f), \theta(3, f) - \theta(2, f), \ldots, \theta(t, f) - \theta(t-1, f)$$

Next, a histogram of the phase difference data $\Delta\theta(t, f)$, pdf($\Delta\theta(k, fb)$), was built by using 20 equidistant bins k from -2π to 2π radian and 5 traditional EEG frequency bands, fb, that consists of delta (1–4 Hz), theta (4–8 Hz), alpha (8–13 Hz), beta (13–30 Hz), and gamma (30–50 Hz) bands. Any phase change with $\Delta\theta > \left|\frac{\pi}{5}\right|$ was defined as non-trivial (phase 'discontinuity'), while phase change with $\Delta\theta \in \left[-\frac{\pi}{5}, \frac{\pi}{5}\right]$ was defined as trivial. Finally, the Phase Discontinuity Index for each frequency band was calculated for each frequency band fb (Figure 2; Sanders, 2019; Sanders used the name, Phase Jump Index).

$$Phase\ Discontinuity\ index(fb) = \frac{\sum_{k=1}^{9} \mathrm{pdf}(\Delta\theta(k, fb)) + \sum_{k=12}^{20} \mathrm{pdf}(\Delta\theta(k, fb))}{\sum_{k=10}^{11} \mathrm{pdf}(\Delta\theta(k, fb))}$$

The Phase Discontinuity Index was calculated for 11 IC clusters, 5 frequency bands, and two groups, thus generated 4-D tensor of data 11 × 5 × 2 × (number_of_ICs) where the length of the data in the last term varies for each group and IC cluster. After calculating this frequency-band separated PSD data structure, group differences were tested to generate 11 (clusters) × 5 (frequency bands) result matrix.

2.7. Statistical testing

The group difference was tested for each combination of 11 IC clusters and 5 frequency bands for EEG band power and Phase Discontinuity Index. A general linear model was used to estimate the group difference using Matlab function *fitglme()*. The design matrix included group labels (schizophrenia patients, healthy comparison subjects), age, sex, and use of anxiolytics or anticholinergics [dummy variables were used; patients who were prescribed either anxiolytics or anticholinergics medications = 1 (N=61); patients who were prescribed neither anxiolytics nor anticholinergics medications = 0 (N=87)] so that the influence of the latter three are covaried out as effect of non-interest in testing the group difference; anxiolytics and anticholinergics medications are known to impact resting-state EEG frequency band parameters (Buchsbaum et al., 1985; Sloan et al., 1992). For comparison of cognitive function between groups, independent *t*-tests were used. Correlations between cognitive dysfunction and abnormal EEG band power as well as abnormal Phase Discontinuity Index in estimated source locations in schizophrenia patients were calculated. Because ICA is a data-driven approach, there could be zero, one, or more than one IC contribution(s) to a cluster. If there was no IC contribution to the selected cluster, that subject was excluded from the subsequent correlation analysis. If there were multiple IC contributions, the mean value was calculated across the multiple ICs to serve as the subject's representative value. To address multiple comparison correction, a false discovery rate was used (Yekutieli and Benjamini, 2001).

3. Results

3.1. Estimated source locations of resting-state EEG activity

Eleven contributing IC clusters of resting-state EEG activity are shown in Figure 3. The 11 clusters included the right anterior cingulate gyrus, the left middle cingulate gyrus, the right posterior cingulate gyrus, the right and left supplementary motor area, the right middle temporal gyrus, the left middle temporal pole, the right and left fusiform gyri, the left postcentral gyrus, and a region near the right calcarine sulcus.

3.2. EEG band power in 11 estimated source locations

Power spectral density in 11 estimated source locations is shown in Figure 3. Delta-band power was significantly higher in schizophrenia patients relative to healthy comparison subjects in the right posterior cingulate gyrus ($\beta = 0.34$, $p = 1.2\times10^{-3}$) and the right supplementary motor area ($\beta = 0.26$, $p = 1.0\times10^{-2}$; Supplementary Table 1). Theta-band power was significantly higher in patients in the right posterior cingulate gyrus ($\beta = 0.49$, $p = 2.0\times10^{-6}$), the right supplementary motor area ($\beta = 0.49$, $p = 1.3\times10^{-6}$), the right middle temporal gyrus ($\beta = 0.36$, $p = 1.1\times10^{-2}$), the left middle temporal pole ($\beta = 0.39$, $p = 2.4\times10^{-3}$), the left fusiform gyrus ($\beta = 0.45$, $p = 1.4\times10^{-4}$), and the left postcentral gyrus ($\beta = 0.34$, $p = 3.1\times10^{-3}$). Alpha-band power was significantly higher in patients in the right posterior cingulate gyrus ($\beta = 0.40$, $p = 1.0\times10^{-4}$) and the left supplementary motor area ($\beta = 0.30$, $p = 4.0\times10^{-3}$). Beta-band power was significantly higher in patients in the right posterior cingulate gyrus ($\beta = 0.45$, $p = 1.3\times10^{-5}$) and the right middle temporal gyrus ($\beta = 0.38$, $p = 7.2\times10^{-3}$). Gamma-band power was significantly higher in patients in the right supplementary motor area ($\beta = 0.33$, $p = 1.0\times10^{-3}$), the right middle temporal gyrus ($\beta = 0.41$, $p = 3.7\times10^{-3}$), the left middle temporal pole ($\beta = 0.35$, $p = 6.7\times10^{-3}$), the left fusiform gyrus ($\beta = 0.32$, $p = 7.0\times10^{-3}$), and a region near the right calcarine sulcus ($\beta = 0.34$, $p = 2.3\times10^{-3}$).

Visual examination of PSD in Figure 3 suggested a lower alpha peak frequency in schizophrenia patients. Post hoc analysis of peak alpha frequency and amplitude was performed.

3.3. Post hoc peak frequency and amplitude in alpha-band (8–13 Hz)

In order to quantify and evaluate the effect of the alpha peak shift in PSD, the first-order derivative of PSD was calculated. Next, positive and negative peaks in the alpha range, which was slightly extended to 7–14 Hz to capture marginal cases, were identified. The number of those ICs that have the peak within the alpha range was counted. For these ICs, the peak frequency and peak power were measured. For all clusters and groups and a 3-D tensor of data 11 × 2 × (number_of_ICs) for peak frequency in Hz and peak power in 10*log10 ($\mu V^2/Hz$) in dB was generated. The group difference was tested for each cluster to yield a vector of 11 (clusters) values. A general linear model was used to estimate the group difference using the design matrix included group labels (schizophrenia patients, healthy comparison subjects), age, sex, and use of anxiolytics or anticholinergics.

The peak frequency of alpha was significantly lower in schizophrenia patients compared to healthy subjects in the left middle cingulate gyrus (β= −0.68, p= 1.1×10^{-2}), the left middle temporal pole (β= −0.56, p= 2.6×10^{-3}), the right fusiform gyrus (β= − 0.43, p= 1.5×10^{-2}), and the left fusiform gyrus (β= −0.40, p= 1.5×10^{-2}; Supplementary Table 2). No peak power was significantly different between the groups (Supplementary Table 3).

3.4. Phase Discontinuity Index

Phase Discontinuity Indices of alpha-band EEG activity in the right middle temporal gyrus (β= 0.40, p= 3.0×10^{-3}) and the left middle temporal pole (β= 0.45, p= 1.3×10^{-3}) were significantly higher in patients (Figure 4, Supplementary Table 4). Phase Discontinuity Indices of theta-band EEG activity in the right posterior cingulate gyrus (β= −0.31, p= 2.9×10^{-3}), the left middle temporal pole (β= −0.60, p= 2.6×10^{-6}), and the left fusiform gyrus (β= −0.36, p= 2.0×10^{-3}) were significantly lower in schizophrenia patients compared to healthy subjects.

3.5. Correlation analyses

Working memory (t_{288}= −8.0, p= 3.1×10^{-14}) and verbal memory performance (t_{287}= − 8.5, p= 1.1×10^{-15}) were significantly lower in schizophrenia patients relative to healthy comparison subjects. Theta-band power in the right middle temporal gyrus (r= −0.36, p= 1.2×10^{-3}) and the left postcentral cortex (r= −0.27, p= 2.9×10^{-3}) was significantly correlated with verbal memory impairment in schizophrenia patients (Supplementary Table 5, Supplementary Figure 1). The significance remained after adjusted to age, sex, and use of anxiolytics or anticholinergics (the right middle temporal gyrus, standardized β= −0.29, p= 8.4×10^{-3}; the left postcentral cortex, β= −0.23, p= 1.2×10^{-2}; uncorrected p< 0.05). For supplementary information, we performed additional correlation analyses between verbal memory performance and theta-band power in the right middle temporal gyrus (r= 0.03, p= 0.83) and the left postcentral cortex (r= 0.03, p= 0.79) in healthy comparison subjects; there was no significant correlation between them.

There were no significant correlations between cognitive function and Phase Discontinuity Index in schizophrenia patients (Supplementary Table 6).

4. Discussion

To our knowledge, this is the first investigation of phase discontinuity of resting-state frequency oscillations within cortical sources in schizophrenia patients. Patients showed abnormal elevations of EEG power across multiple independent brain regions, including the temporal region (the middle temporal gyrus, the middle temporal pole, and the fusiform gyrus) in the theta, beta, and gamma-bands as well as the posterior cingulate gyrus in the delta, theta, alpha, and beta-bands. The higher theta-band power in the middle temporal gyrus was significantly correlated with cognitive dysfunction in schizophrenia patients. The peak frequency of alpha was lower in schizophrenia patients in the middle cingulate gyrus, the middle temporal pole, and the fusiform gyrus. Furthermore, patients also showed a significantly higher rate of alpha phase discontinuity in the middle temporal gyrus and the

middle temporal pole, as well as a lower rate of theta phase discontinuity in the middle temporal pole, the fusiform gyrus, and the posterior cingulate gyrus.

4.1. Abnormal elevations of resting-state EEG power

The abnormal elevations of EEG power across multiple bands such as delta, theta, alpha, and beta in schizophrenia patients were consistent with previous studies (Narayanan et al., 2014; Newson and Thiagarajan, 2018). For gamma-bands, previous findings of the gamma-band power elevation in the left temporal and medial posterior regions were also seen in the current study (Bandyopadhyaya et al., 2011; Grent-'t-Jong et al., 2018).

Notably, our findings were highly consistent with functional magnetic resonance imaging (fMRI) default mode network abnormalities in schizophrenia patients; the brain regions such as the ventral medial prefrontal cortex and the posterior cingulate cortex are thought to feature in the default mode network (Buckner et al., 2008; Whitfield-Gabrieli and Ford, 2012). Greater resting-state EEG power in the posterior cingulate gyrus is consistent with greater default mode network activation in schizophrenia. This similarity is remarkable, given the pronounced differences in temporal resolution between neural activity reflected via the blood oxygenation-dependent (BOLD) hemodynamic response and electrical activity recorded by resting-state EEG (Garrity et al., 2007).

4.2. Alpha slowing

The present results also have implications for a more nuanced understanding of alpha abnormalities in schizophrenia. It is generally expected the PSD of mammalian EEG typically follows a 1/f curve with a peak within the alpha band (8–13 Hz; Nunez and Srinivasan, 2006). The leftward shift of this alpha peak has been referred to as alpha slowing. Results of post hoc analyses in the alpha peak analysis, in which the frequency was lower in schizophrenia patients, were consistent with previous findings of decreased scalp peak alpha frequency in individuals with first-episode psychosis (Murphy and Öngür, 2019). The decreased peak alpha frequency quantified from independent contributing neural sources in chronic schizophrenia patients in the present study demonstrates that this abnormality is broadly distributed across multiple brain regions, including the cingulate, somatosensory, temporal, and occipital cortices. The widespread and robust nature of alpha slowing in schizophrenia patients thus warrants further investigation as a novel target to investigate the pathophysiology of schizophrenia.

4.3. Abnormal phase discontinuity rate

Despite widespread resting-state abnormalities across 5 frequency bands and 11 brain regions in schizophrenia patients, it is surprising that only 5 relatively circumscribed discontinuities in phase oscillations were detected. Since waveform amplitudes and shapes are likely associated with neuronal firing patterns, increased biological noise, reduced signal propagation, and disrupted circuitry may provide a mechanistic accounting of phase discontinuities (Uhlhaas and Singer, 2010; Winterer et al., 2004; Winterer et al., 2000). Although our results did not show any correlations with clinical variables, Winterer et al. showed a negative correlation between the prefrontal noise and working memory performance in schizophrenia patients (Winterer et al., 2004). In this context, phase

discontinuities may be recurring, and waveform irregularities may be prolonged. A higher rate of phase discontinuity may not simply be a marker of neural inefficiency as its function may vary by location and band. Although speculative, it is also possible that the increased alpha phase discontinuity in schizophrenia reflects a mechanism to compensate for impairments in auditory information processing because the abnormality was found in the temporal regions including the auditory cortex; further investigation of the neuronal and circuit-level mechanisms underlying the phase discontinuities is therefore warranted.

4.4. Limitations

Results in this study should be considered in the context of several limitations. First, this is a cross-sectional cohort study of a heterogeneous sample of schizophrenia patients, the majority of whom were receiving complex medication regimens. While we adjusted for effects of anxiolytics and anticholinergics using dummy variables, it is possible that other medications or patient acuity may contribute to phase discontinuity of resting-state EEG activity. Carefully controlled randomized controlled trials are needed to disentangle medication effects. Second, schizophrenia and healthy comparison groups were not matched on age or sex. Although we regressed out the effects of age and sex in the statistical analyses, the effect might be not eliminated completely. Third, only 40 EEG channels were used for the analyses in this study. The use of higher density recordings with at least 64 channels (Light and Swerdlow, 2020), individual MRI data, and digitized scalp sensor locations will likely yield improved accuracy of source locations. Fourth, as in other studies of patients with a well-established illness; findings may not generalize to at-risk or early-illness psychosis patients. Nevertheless, studying patients with established illness may help clarify prominent characteristics of phase discontinuity index that may be subtler or even absent in risk or early-illness psychosis patients.

4.5. Conclusion

In this study, we report for the first time a comprehensive characterization of phase discontinuity in schizophrenia, which included abnormalities across multiple brain regions across multiple frequency bands. Patients showed abnormal elevations of EEG power in the temporal region and the posterior cingulate gyrus in multiple bands. The higher theta-band power in the middle temporal gyrus was correlated with verbal memory impairment in patients. The peak frequency of alpha was lower in patients in the cingulate gyrus and temporal regions. Investigation of the neural mechanisms underlying abnormal resting-state EEG activity and phase discontinuity may clarify core pathophysiologic abnormalities in schizophrenia, explain higher-order and emergent cognitive abnormalities, and advance novel therapeutic development.

Supplementary Material

Refer to Web version on PubMed Central for supplementary material.

Acknowledgements

We gratefully acknowledge all the participants of this study.

Role of funding source

This study was supported by JSPS Overseas Research Fellowships (D. K), the Sidney R. Baer, Jr. Foundation, the Brain and Behavior Research Foundation, grants from NIMH (MH79777, MH042228; G.A.L, D.L.B) and the VISN-22 Mental Illness, Research, Education, and Clinical Center. Swartz Center for Computational Neuroscience is supported by generous gift of Swartz Foundation (New York).

References

Bandyopadhyaya D, Nizamie SH, Pradhan N, Bandyopadhyaya A, 2011. Spontaneous gamma coherence as a possible trait marker of schizophrenia-An explorative study. Asian J Psychiatr 4(3), 172–177. [PubMed: 23051113]

Baradits M, Kakuszi B, Bálint S, Fullajtár M, Mód L, Bitter I, Czobor P, 2019. Alterations in resting-state gamma activity in patients with schizophrenia: a high-density EEG study. Eur Arch Psychiatry Clin Neurosci 269(4), 429–437. [PubMed: 29569047]

Blum S, Jacobsen NSJ, Bleichner MG, Debener S, 2019. A Riemannian Modification of Artifact Subspace Reconstruction for EEG Artifact Handling. Front Hum Neurosci 13, 141. [PubMed: 31105543]

Buchsbaum MS, Hazlett E, Sicotte N, Stein M, Wu J, Zetin M, 1985. Topographic EEG changes with benzodiazepine administration in generalized anxiety disorder. Biol Psychiatry 20(8), 832–842. [PubMed: 2862924]

Buckner RL, Andrews-Hanna JR, Schacter DL, 2008. The brain's default network: anatomy, function, and relevance to disease. Ann N Y Acad Sci 1124, 1–38. [PubMed: 18400922]

Chang CY, Hsu SH, Pion-Tonachini L, Jung TP, 2018. Evaluation of Artifact Subspace Reconstruction for Automatic EEG Artifact Removal. Conf Proc IEEE Eng Med Biol Soc 2018, 1242–1245.

Chang CY, Hsu SH, Pion-Tonachini L, Jung TP, 2020. Evaluation of Artifact Subspace Reconstruction for Automatic Artifact Components Removal in Multi-channel EEG Recordings. IEEE Trans Biomed Eng 67, 1114–1121. [PubMed: 31329105]

Collins DL, Neelin P, Peters TM, Evans AC, 1994. Automatic 3D intersubject registration of MR volumetric data in standardized Talairach space. J Comput Assist Tomogr 18(2), 192–205. [PubMed: 8126267]

Crowe SF, 2000. Does the letter number sequencing task measure anything more than digit span? Assessment 7(2), 113–117. [PubMed: 10868248]

da Cruz JR, Favrod O, Roinishvili M, Chkonia E, Brand A, Mohr C, Figueiredo P, Herzog MH, 2020. EEG microstates are a candidate endophenotype for schizophrenia. Nat Commun 11(1), 3089. [PubMed: 32555168]

Delis DC, Kramer JH, Kaplan E, Ober BA, 2000. California Verbal Learning Test–second edition (CVLT-II). Psychological Corporation, San Antonio, TX.

Delorme A, Makeig S, 2004. EEGLAB: an open source toolbox for analysis of single-trial EEG dynamics including independent component analysis. J Neurosci Methods 134(1), 9–21. [PubMed: 15102499]

Gabard-Durnam LJ, Mendez Leal AS, Wilkinson CL, Levin AR, 2018. The Harvard Automated Processing Pipeline for Electroencephalography (HAPPE): Standardized Processing Software for Developmental and High-Artifact Data. Front Neurosci 12, 97. [PubMed: 29535597]

Galuske RAW, Munk MHJ, Singer W, 2019. Relation between gamma oscillations and neuronal plasticity in the visual cortex. Proc Natl Acad Sci U S A 116(46), 23317–23325. [PubMed: 31659040]

Garrity AG, Pearlson GD, McKiernan K, Lloyd D, Kiehl KA, Calhoun VD, 2007. Aberrant "default mode" functional connectivity in schizophrenia. Am J Psychiatry 164(3), 450–457. [PubMed: 17329470]

Grent-'t-Jong T, Gross J, Goense J, Wibral M, Gajwani R, Gumley AI, Lawrie SM, Schwannauer M, Schultze-Lutter F, Navarro Schröder T, Koethe D, Leweke FM, Singer W, Uhlhaas PJ, 2018. Resting-state gamma-band power alterations in schizophrenia reveal E/I-balance abnormalities across illness-stages. Elife 7.

Hagoort P, Hald L, Bastiaansen M, Petersson KM, 2004. Integration of word meaning and world knowledge in language comprehension. Science 304(5669), 438–441. [PubMed: 15031438]

Hirano Y, Oribe N, Kanba S, Onitsuka T, Nestor PG, Spencer KM, 2015. Spontaneous Gamma Activity in Schizophrenia. JAMA Psychiatry 72(8), 813–821. [PubMed: 25587799]

Joliot M, Ribary U, Llinas R, 1994. Human oscillatory brain activity near 40 Hz coexists with cognitive temporal binding. Proc Natl Acad Sci U S A 91(24), 11748–11751. [PubMed: 7972135]

Koshiyama D, Miyakoshi M, Tanaka-Koshiyama K, Joshi YB, Molina JL, Sprock J, Braff DL, Light GA, 2020. Neurophysiologic Characterization of Resting State Connectivity Abnormalities in Schizophrenia Patients. Front Psychiatry 11, 608154. [PubMed: 33329160]

Kothe CA, Makeig S, 2013. BCILAB: a platform for brain-computer interface development. J Neural Eng 10(5), 056014. [PubMed: 23985960]

Light GA, Swerdlow NR, 2020. Selection criteria for neurophysiologic biomarkers to accelerate the pace of CNS therapeutic development. Neuropsychopharmacology 45(1), 237–238. [PubMed: 31506611]

Miltner WH, Braun C, Arnold M, Witte H, Taub E, 1999. Coherence of gamma-band EEG activity as a basis for associative learning. Nature 397(6718), 434–436. [PubMed: 9989409]

Mullen TR, Kothe CA, Chi YM, Ojeda A, Kerth T, Makeig S, Jung TP, Cauwenberghs G, 2015. Real-Time Neuroimaging and Cognitive Monitoring Using Wearable Dry EEG. IEEE Trans Biomed Eng 62(11), 2553–2567. [PubMed: 26415149]

Murphy M, Öngür D, 2019. Decreased peak alpha frequency and impaired visual evoked potentials in first episode psychosis. Neuroimage Clin 22, 101693. [PubMed: 30825710]

Narayanan B, O'Neil K, Berwise C, Stevens MC, Calhoun VD, Clementz BA, Tamminga CA, Sweeney JA, Keshavan MS, Pearlson GD, 2014. Resting state electroencephalogram oscillatory abnormalities in schizophrenia and psychotic bipolar patients and their relatives from the bipolar and schizophrenia network on intermediate phenotypes study. Biol Psychiatry 76(6), 456–465. [PubMed: 24439302]

Newson JJ, Thiagarajan TC, 2018. EEG Frequency Bands in Psychiatric Disorders: A Review of Resting State Studies. Front Hum Neurosci 12, 521. [PubMed: 30687041]

Nolte G, Bai O, Wheaton L, Mari Z, Vorbach S, Hallett M, 2004. Identifying true brain interaction from EEG data using the imaginary part of coherency. Clin Neurophysiol 115(10), 2292–2307. [PubMed: 15351371]

Nunez P, Srinivasan R, 2006. Electric Fields of the Brain. Oxford University Press, New York.

Olhede SC, Walden AT, 2002. IEEE Transactions on Signal Processing 50(11), 2661–2670.

Oostenveld R, Fries P, Maris E, Schoffelen JM, 2011. FieldTrip: Open source software for advanced analysis of MEG, EEG, and invasive electrophysiological data. Comput Intell Neurosci 2011, 156869. [PubMed: 21253357]

Oostenveld R, Praamstra P, 2001. The five percent electrode system for high-resolution EEG and ERP measurements. Clin Neurophysiol 112(4), 713–719. [PubMed: 11275545]

Piazza C, Miyakoshi M, Akalin-Acar Z, Cantiani C, Reni G, Bianchi AM, 2016. An Automated Function for Identifying EEG Independent Components Representing Bilateral Source Activity, XIV Mediterranean Conference on Medical and Biological Engineering and Computing 2016. Springer International Publishing, 105–109.

Pion-Tonachini L, Kreutz-Delgado K, Makeig S, 2019. ICLabel: An automated electroencephalographic independent component classifier, dataset, and website. Neuroimage 198, 181–197. [PubMed: 31103785]

Rodriguez E, George N, Lachaux JP, Martinerie J, Renault B, Varela FJ, 1999. Perception's shadow: long-distance synchronization of human brain activity. Nature 397(6718), 430–433. [PubMed: 9989408]

Rousseeuw P, 1987. Silhouettes: a graphical aid to the interpretation and validation of cluster analysis. J Comput Appl Math 20, 53–65.

Sanders TH, 2019. Phase discontinuities underlie increased drowsiness and diminished sleep quality in older humans. BioRxiv, doi: 10.1101/696658.

Sloan EP, Fenton GW, Standage KP, 1992. Anticholinergic drug effects on quantitative electroencephalogram, visual evoked potential, and verbal memory. Biol Psychiatry 31(6), 600–606. [PubMed: 1581439]

Spellman T, Rigotti M, Ahmari SE, Fusi S, Gogos JA, Gordon JA, 2015. Hippocampal-prefrontal input supports spatial encoding in working memory. Nature 522(7556), 309–314. [PubMed: 26053122]

Tanaka-Koshiyama K, Koshiyama D, Miyakoshi M, Joshi YB, Molina JL, Sprock J, Braff DL, Light GA, 2020. Abnormal spontaneous gamma power is associated with underlying verbal learning and memory dysfunction in schizophrenia. Front Psychiatry 11, 832. [PubMed: 33110410]

Tikka SK, Yadav S, Nizamie SH, Das B, Tikka DL, Goyal N, 2014. Schneiderian first rank symptoms and gamma oscillatory activity in neuroleptic naïve first episode schizophrenia: a 192 channel EEG study. Psychiatry Investig 11(4), 467–475.

Traub RD, Whittington MA, Stanford IM, Jefferys JG, 1996. A mechanism for generation of long-range synchronous fast oscillations in the cortex. Nature 383(6601), 621–624. [PubMed: 8857537]

Uhlhaas PJ, Singer W, 2010. Abnormal neural oscillations and synchrony in schizophrenia. Nat Rev Neurosci 11(2), 100–113. [PubMed: 20087360]

Whitfield-Gabrieli S, Ford JM, 2012. Default mode network activity and connectivity in psychopathology. Annu Rev Clin Psychol 8, 49–76. [PubMed: 22224834]

Winterer G, Coppola R, Goldberg TE, Egan MF, Jones DW, Sanchez CE, Weinberger DR, 2004. Prefrontal broadband noise, working memory, and genetic risk for schizophrenia. Am J Psychiatry 161(3), 490–500. [PubMed: 14992975]

Winterer G, Ziller M, Dorn H, Frick K, Mulert C, Wuebben Y, Herrmann WM, Coppola R, 2000. Schizophrenia: reduced signal-to-noise ratio and impaired phase-locking during information processing. Clin Neurophysiol 111(5), 837–849. [PubMed: 10802455]

Yekutieli D, Benjamini Y, 2001. The control of the false discovery rate in multiple testing under dependency. The Annals of Statistics 29(4), 1165–1188.

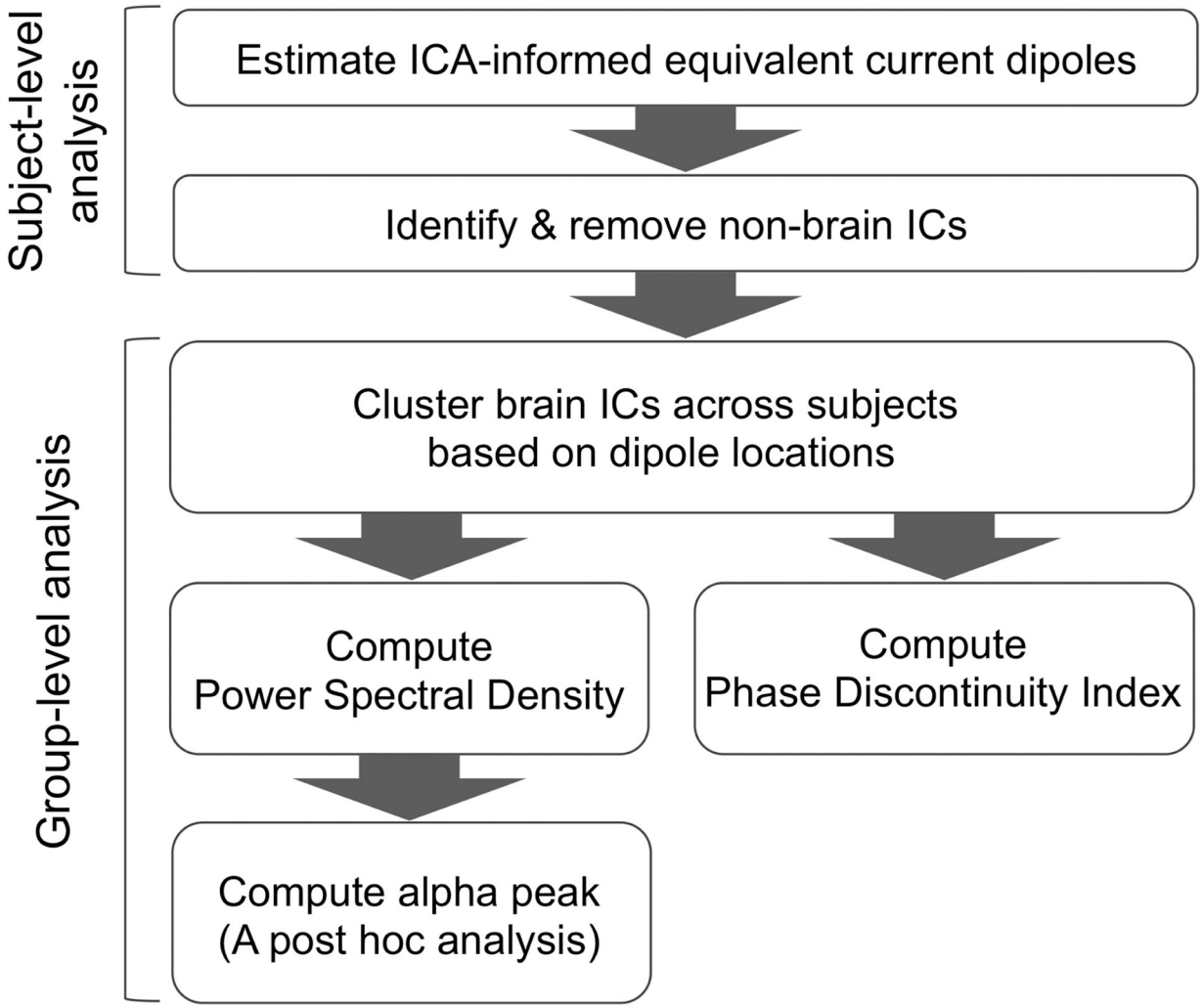

Figure 1.
Procedures of the source-level EEG analysis. Abbreviation: EEG, electroencephalogram; ICs, independent components; ICA, independent component analysis.

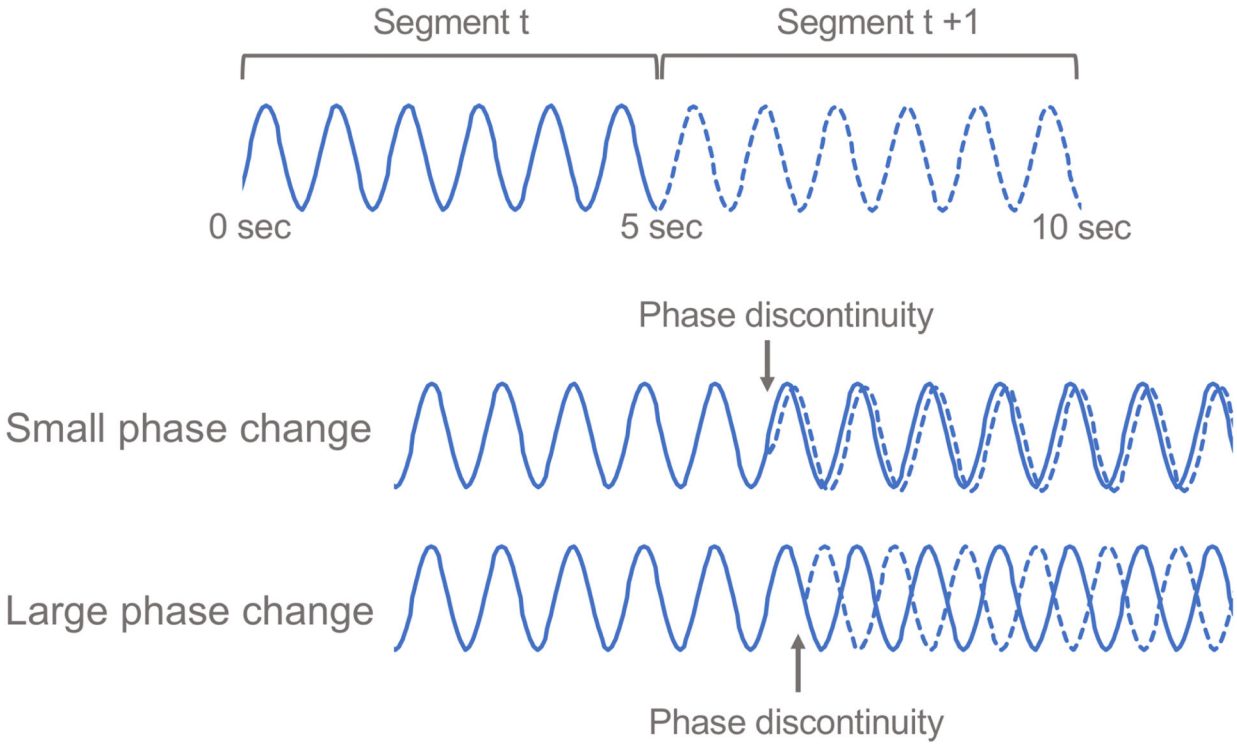

Figure 2. Phase Discontinuity Index.

Phase Discontinuity Index is a ratio of (large phase change between segment t and segment t +1)/(small phase change between segment t and segment t+1).

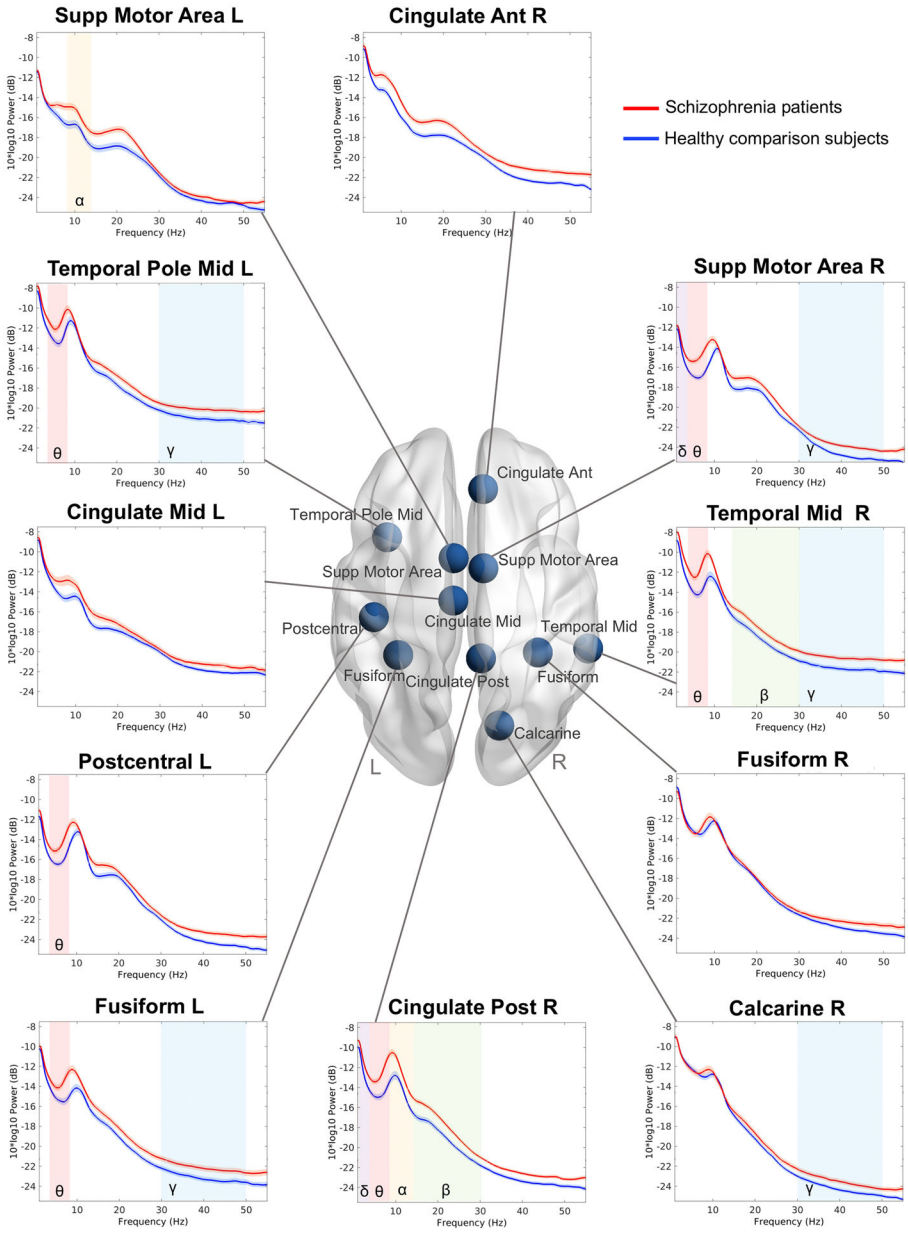

Figure 3. EEG band power in 11 estimated source locations.

The power spectral density of healthy subjects and schizophrenia patients in 11 estimated source locations is shown. The significant difference of EEG band power between the groups was colored ($p < 0.05$, a false discovery rate corrected). Blue or red color shade along the power spectral density indicates a standard error in patients with schizophrenia and healthy comparison subjects, respectively. Abbreviation: Ant, anterior; EEG, electroencephalogram; L, left; Mid, middle; Post, posterior; R, right; Supp, supplementary.

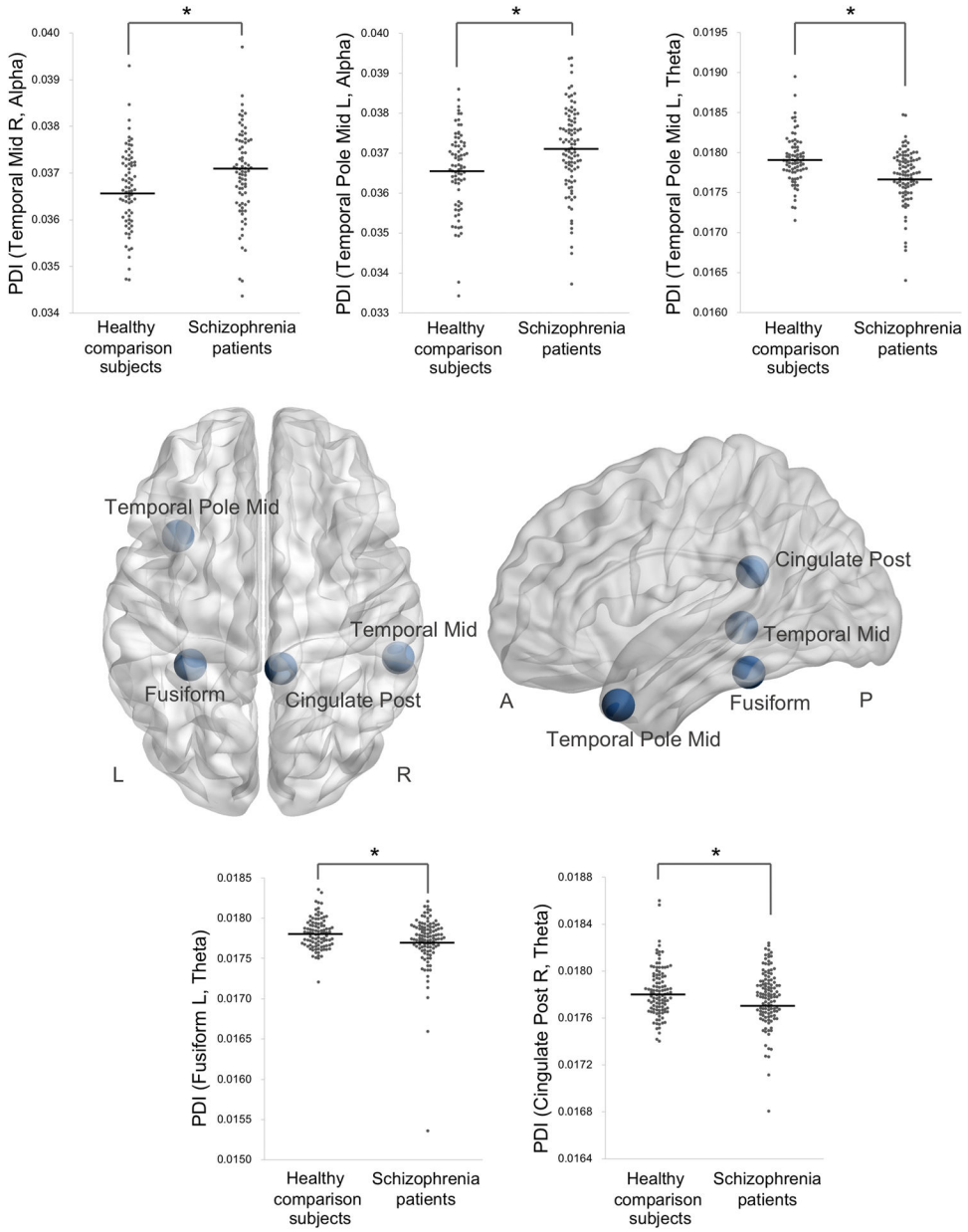

Figure 4. Phase Discontinuity Indices (PDI) that are significantly different between patients with schizophrenia and healthy comparison subjects.

The black horizontal line indicates the means of the PDI. Asterisks indicate a statistically significant difference in PDI between patients with schizophrenia and healthy comparison subjects ($p < 0.05$, a false discovery rate corrected). Abbreviation: A, anterior; HCS, healthy comparison subjects; L, left; Mid, middle; P, posterior; R, right; Supp, supplementary; SZ, schizophrenia.

Table 1

Demographic data of subjects

	Healthy comparison subjects N=143	Schizophrenia patients N=148
Gender (Male/Female)	67/76	97/51
Age (year)	39.6 (13.0)	46.2 (10.9)
Duration of illness (year)		25.4 (11.8)
SAPS		6.7 (4.0)
SANS		16.9 (3.8)
GAF		41.1 (4.4)

Two subjects have no data of duration of illness; One subjects have no SAPS or SANS data.

Abbreviations: SAPS, Scale for the Assessment of Positive Symptoms; SANS, Scale for the Assessment of Negative Symptoms; GAF, Global Assessment of Functioning.